

## Evidence for threshold effects in positron diffraction from NaF and LiF

T. N. Horsky, G. R. Brandes, K. F. Canter, and P. H. Lippel\*  
*Brandeis University, Waltham, Massachusetts 02154*

A. P. Mills, Jr.  
*AT&T Bell Laboratories, Murray Hill, New Jersey 07974*  
 (Received 20 March 1989)

We have measured the energy dependence of the intensity of a positron beam specularly reflected from the (100) surfaces of NaF and LiF. A 1-eV-wide peak located at an energy that decreases with increasing angle of incidence  $\theta$  is qualitatively identified as a beam threshold effect. Given the known small positron affinity for the solids, the narrowness of the peak is consistent with its being due to a true surface resonance. However, the dispersion appears to depart from the expected energy versus  $\theta$  trajectory parallel to the kinematic threshold. Additionally, a search in 50-meV steps did not reveal any fine structure in the peaks, possibly due to our 0.3-eV effective instrumental resolution. Further experiments to map the dispersion with greater precision, to measure the binding energies of the resonances, and to search for possible fine structure are proposed.

### I. INTRODUCTION

In a low-energy electron diffraction (LEED) experiment a monoenergetic electron beam is incident on a crystal surface at a fixed angle  $\theta$  and one measures the positions and intensities of various diffracted beams.<sup>1</sup> As the electron energy  $E$  is increased starting from zero, one at first observes only a specular beam. At certain threshold energies determined by the two-dimensional (2D) geometry of the surface diffracted beams appear on the horizon, emerging from the crystal at a grazing angle with respect to the surface. It was recognized some time ago that just below a threshold energy one might have the conditions for populating a traveling-wave electron surface state.<sup>2-4</sup> Since the wave would couple weakly to the incident beam, it would appear in the specularly reflected beam as a narrow-energy resonance. A study of such surface resonances would be interesting because their dispersion would reveal the perpendicular binding energies and would give us information about the 2D periodic potential felt by a particle moving along the surface.

Small peaks in the intensity of the specular beam are often observed just before the emergence of new beams, but after many years of study there is general agreement that in the case of metallic surfaces they are caused by multiple scattering interference of waves that are not necessarily confined to the surface.<sup>5,6</sup> Unfortunately, the purely surface resonance does not seem to occur because in general electrons have a large attraction for the crystal. An exception to this rule would be expected to occur for some wide-band-gap solids, such as the alkali halides and the rare gases, which have a small electron affinity. Although such materials may have a large negative inner potential, the only available states for scattering are above the band gap. Positrons have only a small or even negative affinity for many solids<sup>7</sup> and true surface reso-

nances should be common. We are thus prompted to search for grazing emergence threshold effects in low-energy positron diffraction (LEPD).<sup>8</sup> Although there have been several theoretical predictions<sup>9,10</sup> of threshold effects in LEPD, they have not been experimentally confirmed.

The calculated grazing emergence threshold energies are given by

$$E_{nm} = \frac{\hbar^2}{2m} (\mathbf{k}_{\parallel} + \mathbf{G}_{nm})^2, \quad (1)$$

where  $\mathbf{k}_{\parallel}$  is the projection of the incident positron wave vector on the surface. The  $\mathbf{G}_{nm}$  are the reciprocal net vectors of the surface,  $\mathbf{G}_{nm} = (2\pi/a)(n\hat{\mathbf{e}}_1 + m\hat{\mathbf{e}}_2)$ , where the  $\hat{\mathbf{e}}_i$  are unit vectors in the  $\langle 11 \rangle$  and  $\langle 1\bar{1} \rangle$  directions,  $a = d/\sqrt{2}$ , and  $d$  is the conventional face-centered-cubic unit cell dimension. In terms of the angle of incidence  $\theta$ ,  $k_{\parallel} = k \sin(\theta)$ , and the azimuthal angle  $\phi$  of  $\mathbf{k}_{\parallel}$  relative to the  $\langle 10 \rangle$  direction, the threshold energies are

$$E_{nm} = E_0 \sec^4(\theta) \{ f \sin\theta + [f^2 \sin^2\theta + (n^2 + m^2) \cos^2\theta]^{1/2} \}^2, \quad (2)$$

where  $f = \sqrt{1/2}[(n+m)\cos\phi + (n-m)\sin\phi]$  and  $E_0 = 4\pi^2\hbar^2/ma^2 = 14.08$  eV for NaF and 18.60 eV for LiF.

A surface resonance is a metastable surface state having a significant amplitude for being found in the vacuum. The wave function is a 2D Bloch state for a particle of effective mass  $m^*$  with an energy  $\epsilon_j(\mathbf{k}_{\parallel})$  determined by the solutions of the Schrödinger equation in the presence of a 2D-periodic 3D crystal potential. In the simplest case, the potential is separable into a 2D periodic part,  $V(x, y)$ , and a potential well perpendicular to the surface. The solutions for different values of  $j$  have energies differing from the threshold energy by the binding energies  $E_j$  for the particle in the well.

The minimum requirement for the existence of a surface resonance, that the particle see a band gap for negative energies associated with motion perpendicular to the surface, is satisfied for positrons and electrons interacting with NaF and LiF where the affinities are on the order of 0.5 eV.<sup>11</sup> We can argue that  $V(x,y)$  is small for electrons for the same reasons that make the nearly-free-electron model successful.<sup>12</sup> The surface resonances will thus be found at energies  $E = E_{nm} - E_j$ . If the potential is not weak, as might be the case for positrons, the resonances could be found at energies  $E = \epsilon_j(\mathbf{k}_{\parallel} + \mathbf{G}_{nm})$  much different from  $E_{nm} - E_j$ .

## II. EXPERIMENT

We have chosen to examine two alkali halides, NaF and LiF, partly because they have been studied in detail using LEED.<sup>2,13</sup> A monochromatic positron beam of 2 mm diameter and 1° angular divergence was obtained from a <sup>58</sup>Co positron source and W(110) moderator followed by two stages of brightness enhancement.<sup>14</sup> The samples were cleaved in air and mounted in a vacuum chamber equipped with a precision goniometer, a display LEED system, and a digital position-sensitive detector for measuring the intensity of the specularly reflected positron beam. We did nothing to prepare the surfaces, except to heat them in vacuum, and keep them at a temperature of 130°C to prevent charging. In lieu of analysis of the surfaces by Auger spectroscopy, we relied on the report that air-cleaved samples of LiF and NaF show only submonolayer levels of contamination by O and C when examined in an ultrahigh-vacuum system.<sup>15</sup> A schematic of the experimental setup is shown in Fig. 1.

Intensity profiles were produced by repeatedly ramping the beam energy in either 0.5 eV or 1 eV increments from 10 to 80 eV and integrating the digitally recorded spot intensities. The multiscaling averaging allowed long collection times, and hence large integrated counts, without deleterious effects due to possible small slow drifts in the beam energy or current. The data were normalized by dividing by the incident beam current, measured as a function of energy by electrostatically mirroring the positron

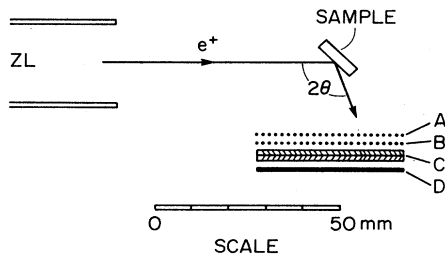


FIG. 1. Experimental geometry. Variable energy positron beam exits the grounded end of an electrostatic zoom lens (ZL) and is specularly reflected at the sample surface through a scattering angle of  $2\theta$ . The scattered beam profile and intensity are monitored by a 40-mm-diam, 2D imaging detector array consisting of a grounded grid, A; a retarding grid, B; a channel electron multiplier array detector, C; and a resistive anode position encoder, D.

beam into the detector array. The polar angle  $\theta$  was systematically varied in the range  $15^\circ \leq \theta \leq 50^\circ$ . We discovered a narrow peak near the  $(\bar{1}\bar{1})$  emergence threshold energy, and mapped its shape in 0.1 eV energy increments. We also measured its centroid energy with 2° changes in  $\theta$  to determine its dispersion. A typical raw intensity profile and detail of the narrow peak are displayed in Fig. 2 for LiF for  $\theta = 25^\circ$ . The large  $n = 2$  Bragg peak occurs at a moderator bias of 10.5 V, and the small-amplitude narrow peak occurs at 17 V. Similar data were obtained at other values of  $\theta$  and also for NaF. Table I lists all the Bragg peaks and narrow peaks recorded. The peak energies are equal to the moderator bias voltage plus an offset  $\Delta V$  to account for the positron negative affinity of W(110) and the difference in contact potentials of W(110) and type 304 stainless steel. We measured  $\Delta V = (2.7 \pm 0.2)$  eV by a retarding field analysis of the positron beam using a 304 stainless steel grid.

Once the dispersions were recorded for LiF and NaF, we attempted to identify fine structure within the narrow peak. Previous LEED measurements of metal surfaces<sup>3-6</sup> as well as dynamical calculations for LEPD (Ref. 10) reveal a Rydberg-like series of intensity maxima contained within a few eV wide envelope as one approaches threshold. The oscillations are due to the long-range image potential well at the surface and are sensitive to the exact form of the surface potential barrier. Accordingly, a 3 eV wide segment of the specular beam in the vicinity of the narrow peak was measured in 50 meV steps to a precision of about 1% for several values of  $\theta$ , as shown in Fig. 3 for NaF. The absence of fine structure in the peak is perhaps due to our relatively large instrumental resolution. We estimate that our beam had a full width at half maximum (FWHM) energy spread<sup>7</sup>  $\Delta E \approx 90$  meV and a FWHM angular divergence  $\Delta\theta \approx 0.9^\circ$  estimated from phase space considerations. Since the theoretical  $(\bar{1}\bar{1})$  peak energy has a slope  $dE_p/d\theta \approx 325$  meV per

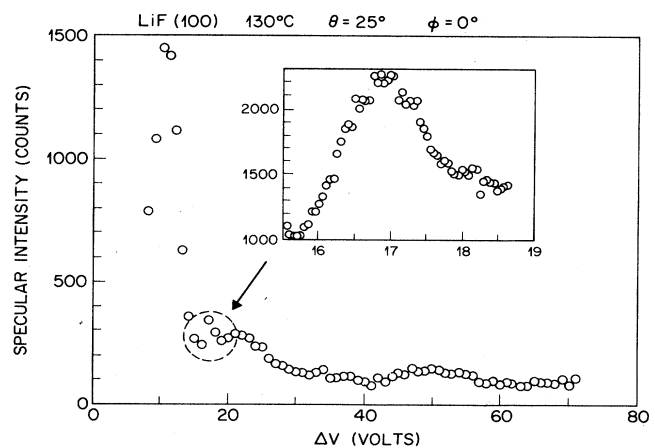


FIG. 2. Intensity of the specular (00) beam for positrons scattered from LiF(100) at a 25° angle of incidence.  $\Delta V$  is the bias voltage between the W(110) moderator and the sample. The inset shows a subsequent detail of the narrow peak. The data in this figure have not been corrected for background or normalized to the incident beam current.

degree, the effective instrumental response function<sup>6</sup> shown inset in Fig. 3 has a FWHM  $[(\Delta\theta)^2(dE_p/d\theta)^2 + (\Delta E)^2]^{1/2} \approx 300$  meV.

The energies of the small amplitude narrow peaks for different values of the angle of incidence  $\theta'$  are shown by the filled circles in Figs. 4 and 5 for LiF and NaF. The angle  $\theta'$  differs from the crystal angle relative to the positron beam because of the contact potential difference  $\Delta\phi_-$  between the sample and the vacuum chamber:  $\theta' = \arctan[\sin\theta/(\cos^2\theta + \Delta\phi_-/E_+)^{1/2}]$ . We have taken  $\Delta\phi_-$  to be that found by Mills and Crane<sup>16</sup> relative to polycrystalline Mo:  $\Delta\phi_- = -1.4$  eV for NaF and  $-0.6$  eV for LiF. The lines in Figs. 4 and 5 are the loci of the lowest order allowed ( $n=2$ ) Bragg peak and the threshold energies  $E_{nm}$  calculated for a weak-scattering crystal surface as a function of  $\theta$  for the nominal value of  $\phi=0$  (solid lines) and for the extreme case  $\phi=10^\circ$  (dashed lines). The locus of empty lattice Bragg-peak energies includes an inner potential  $V_0 = -0.5$  eV for NaF and 0.0 eV for LiF.<sup>11</sup> While there is no reason for the  $n=2$  Bragg peak to lie exactly on the locus, the nearness of the Bragg-peak measurements shown by the open circles gives some confidence in the correctness of the angle and energy scales. We may identify the narrow peaks (filled circle data) with a threshold effect because (1) the peak positions have the negative slope expected for the lowest energy thresholds, (2) they are within a few eV of the  $(\bar{1}\bar{1})$  threshold, and (3) the peaks are narrow compared to the width of the Bragg peaks. However, unlike the peaks observed in LEED for these samples,<sup>2,13</sup> the positron peak

TABLE I. Nominal angle of incidence  $\theta$  and positron energies  $E_+$  at which Bragg peaks and threshold peaks were observed for NaF and LiF (100) surfaces.

Sample	Angle <sup>a</sup>	Bragg peak <sup>b</sup>	Threshold peak <sup>b</sup>
	$\theta$ (deg)	$E_+$ (eV)	$E_+$ (eV)
NaF	15.5±2.0		15.9±0.5
	20		14.9
	22		14.5
	24		14.2
	25.5	9.7±1	14.0
	28.5		13.8
	30.5		13.5
	32.5		13.3
	50.5	18.7±2	
	LiF	23±2.0	12.7±1
25		13.2±0.5	19.7
30		13.7±1	18.7
32		13.7±2	18.7
35		14.7±1	18.2

<sup>a</sup>The angle of incidence of positrons near the sample surface is  $\theta' = \arctan[\sin\theta/(\cos^2\theta + \Delta\phi_-/E_+)^{1/2}]$ , where  $\Delta\phi_- = -1.4$  eV for NaF and  $-0.6$  eV for LiF, and we are assuming that polycrystalline Mo and 304 stainless steel have equal contact potentials.

<sup>b</sup>The peak energies are the moderator bias plus 2.7 eV to account for the positron negative affinity of W(110) and the difference in contact potentials of W(110) and 304 stainless steel.

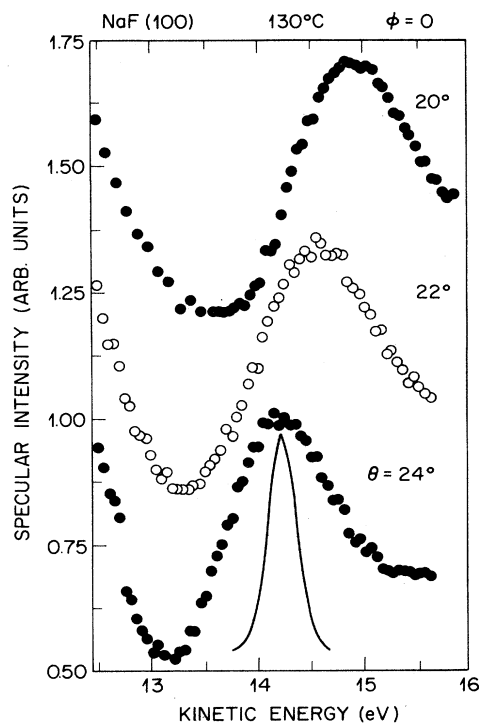


FIG. 3. Normalized specular intensity of the narrow peak as a function of both incident energy and angle of incidence  $\theta$ , illustrating its negative dispersion in energy with increasing values of  $\theta$ . Statistical errors are nominally contained within the plotted points. Peak counts are typically 20000 per point; peak reflectivities are approximately 1%. The instrumental response function, a Gaussian with 0.3 eV full width at half maximum, is shown inset within the bottom peak. The response function is a convolution of a 90 meV natural energy width with a  $0.9^\circ$  beam angular divergence, as discussed in the text.

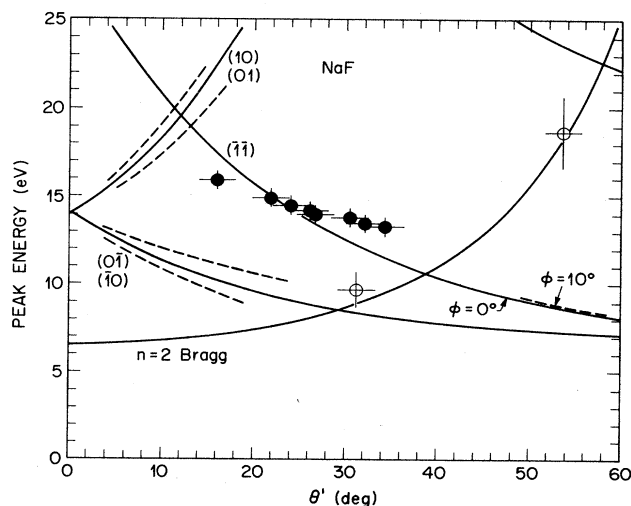


FIG. 4. Energy of the narrow peak vs corrected angle of incidence  $\theta'$  for NaF.

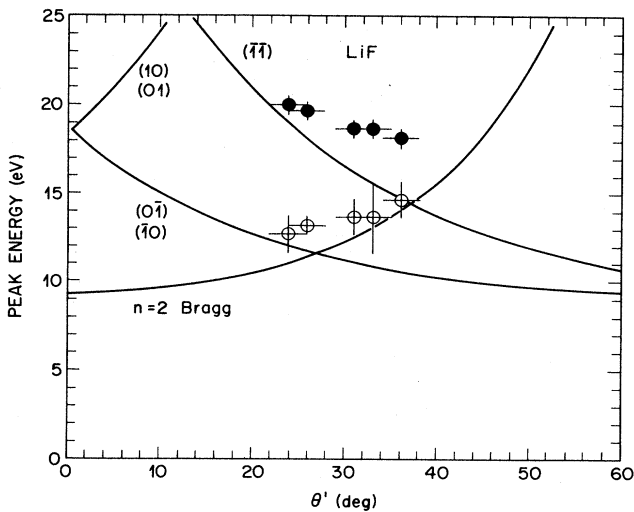


FIG. 5. Energy of the narrow peak vs corrected angle of incidence  $\theta'$  for LiF.

positions appear to not be ascribable to a constant binding energy that causes  $E(\theta)$  to fall on a curve displaced a constant amount from  $E_{nm}$ .

### III. ANALYSIS

We must now attempt to explain why the LEPD and LEED results are so different. A simple analysis would indicate that a surface resonance should lie below its threshold energy, which does not seem to be the case in Figs. 4 and 5. One possibility is that there is an undiscovered systematic error in our measurements of the scattering angle. An analysis of the geometry and mechanism of the sample holder and positron gun leads us to believe that the angle  $\theta$  is known with an error limit of  $\pm 2^\circ$ , whereas a  $10^\circ$ – $15^\circ$  shift in  $\theta$  would be needed to keep the narrow-peak trajectories from crossing the  $(\bar{1}\bar{1})$  threshold. On the other hand, we cannot completely rule out the possibility that stray electromagnetic fields have significantly distorted the positron trajectories. Another possibility is that we are dealing with complicated multiple scattering effects and that a complete calculation including all the proper beams and phase shifts would reproduce the measurements. A large departure from the weak scattering case may thus be the explanation for the distorted dispersion we observe for the narrow LEPD peaks we associate with grazing emergence.

A preliminary investigation of this possibility was carried out by seeing if multiple scattering within a single layer could cause an appreciable departure from the empty-lattice threshold emergence condition. As described in the Appendix, the specular reflection intensity profiles were calculated for a plane wave incident on a 2D sheet of alternating (+) and (–) charges representing the cations and anions. The result is a single narrow (0.5 eV FWHM) peak located 0.4 eV below the empty lattice threshold energies corresponding to the solution of Eq. (1) for the  $(\bar{1}\bar{1})$  beam. We are thus lead to conclude that multiple scattering in a single plane probably does not

cause a large departure from Eq. (1), and does not predict resonance effects above the empty lattice threshold.

One may also raise the possibility of the nature of the surface potential barrier leading to departures from Eq. (1). Indeed, positron reflection from a metal surface as calculated by Read<sup>9</sup> exhibits single peaks above threshold when an asymmetric square well surface is included in dynamical scattering from the bulk-terminated crystal. However, subsequent calculations by Jennings and Nielson<sup>10</sup> using a more realistic, continuously varying, saturated form of the surface barrier displays only fine structure below threshold, analogous to similar results obtained for LEED. Although we are not aware of such investigations for insulating materials, we expect that the magnitude of the image potential will be reduced by the factor  $(\epsilon-1)/(\epsilon+1) \approx 0.8$  for LiF and NaF, and that its saturation close to the surface may depart from the metallic case due to a reduction in the positron-electron correlation energy. Other subjects that should be investigated are (1) the effect of a position-dependent and nondiagonal positron effective-mass tensor caused by polarization of the solid; and (2) the effects of multiple layer scattering, inelastic scattering, positronium formation,<sup>17</sup> and the long-range part of the surface potential.

### IV. CONCLUSION

We have observed narrow features in the positron specular reflection probability that are good candidates for resonances associated with a threshold effect. It would be a good idea in the future to establish the surface sensitivity of the narrow features by attempting to make them go away by modifying the surface conditions of the samples. Further experimentation is needed to map out the line shapes and the  $E$  versus  $\theta$  dispersion with better resolution. Use of a cooled Ni(100) remoderator<sup>18</sup> in conjunction with aperturing of the incident beam angular divergence to  $0.2^\circ$  FWHM would allow an instrumental resolution of 70 meV, sufficient to resolve fine structure associated with excited states and their binding energies. It is to be noted that if the resonances are indeed due to states evanescent in the solid and localized in the potential well outside the surface, they could provide a sensitive probe of overlayers.<sup>10</sup>

### ACKNOWLEDGMENTS

The authors are grateful to D. R. Hamann and E. G. McRae for helpful discussions. This work was supported in part by the National Science Foundation (Grant No. DMR-8519524).

### APPENDIX

It is relatively easy to construct a model with no adjustable parameters that will tell us if multiple scattering in a single layer can cause a gross departure from the empty lattice threshold emergence condition. Whereas previous calculations<sup>9,10</sup> have neglected the 2D periodic part of the "image potential," we suppose that the potential is that due to a 2D array of positive and negative charges,

$$\begin{aligned}
 V(\mathbf{r}) &= e^2 \sum_{n,m} [ |\mathbf{r} - n\hat{\mathbf{e}}_1 - m\hat{\mathbf{e}}_2|^{-1} \\
 &\quad - |\mathbf{r} - (n + \frac{1}{2})\hat{\mathbf{e}}_1 - (m + \frac{1}{2})\hat{\mathbf{e}}_2|^{-1} ] \\
 &= \sum_{\mathbf{G}} V_{\mathbf{G}}(z) \exp(i\mathbf{G} \cdot \mathbf{x}_{\parallel}), \quad (\text{A1})
 \end{aligned}$$

where the  $\hat{\mathbf{e}}_i$  are the primitive unit cell vectors of length  $a$ . The Fourier transform of the potential is

$$V_{\mathbf{G}}(z) = \frac{2\pi e^2 f(\mathbf{G})}{a^2 G} e^{-|zG|}, \quad (\text{A2})$$

where  $f(\mathbf{G}_{nm}) = 1 - (-1)^{n+m}$ . Since the potential is short ranged, we replace it by an equivalent  $\delta$ -function potential,

$$V_{\mathbf{G}} \approx \frac{4\pi e^2 f(\mathbf{G})}{a^2 G^2} \delta(z) = U_{\mathbf{G}} \delta(z). \quad (\text{A3})$$

The 2D Bloch state solutions to the Schrödinger equation with this potential

$$\psi = \sum_{\mathbf{G}} A_{\mathbf{G}}(z) e^{i\mathbf{G} \cdot \mathbf{x}_{\parallel}} e^{ik_{\parallel} \cdot \mathbf{x}_{\parallel}} \quad (\text{A4})$$

have Fourier coefficients

$$A_{\mathbf{G}}(z) = a_{\mathbf{G}} e^{-\alpha_{\mathbf{G}} |z|} \quad (\text{A5})$$

with

$$A_0 = e^{ik_{\perp} z} + a_0 e^{-ik_{\perp} z} \quad (\text{A6})$$

for  $z > 0$  and

$$A_0 = (1 + a_0) e^{ik_{\perp} z} \quad (\text{A7})$$

for  $z < 0$ . The wave numbers are given by

$$\alpha_{\mathbf{G}}^2 = |\mathbf{G} + \mathbf{k}_{\parallel}|^2 - k^2, \quad (\text{A8})$$

and

$$\alpha_0^2 = k_{\parallel}^2 - k^2 = -k_{\perp}^2. \quad (\text{A9})$$

The amplitudes satisfy the matrix equation (in atomic units)

$$\sum_{\mathbf{G}'} (\alpha_{\mathbf{G}} \delta_{\mathbf{G}-\mathbf{G}'} + U_{\mathbf{G}-\mathbf{G}'}') a_{\mathbf{G}'} = -U_{\mathbf{G}}. \quad (\text{A10})$$

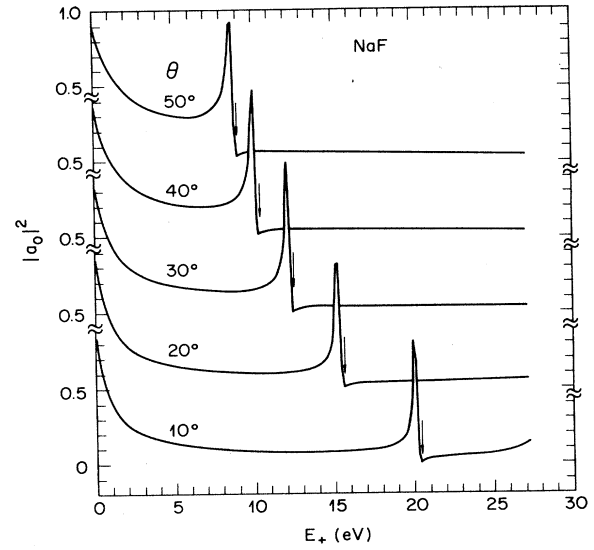


FIG. 6. Specular reflection probability calculated for a single layer of positive and negative point charges at the positions of the ions of an idealized NaF surface. The arrows point to the positions of the resonance peaks in the limit of a very weak potential.

We have truncated Eq. (A2) to include only the amplitudes corresponding to the smallest 25 values of  $\mathbf{G}$ , and solved for the probability of specular reflection,  $|a_0|^2$ , for five values of incident angle  $\theta$ . We learn the following from inspection of the calculated curves in Fig 6. (1) Due to the symmetry of the potential, only the  $(\bar{1}\bar{1})$  resonance is coupled to the scattering particle. (2) There is a zero of the specular reflection probability at the positions of the empty lattice thresholds indicated by the arrows in Fig 6. (3) The resonance peaks are about 0.4 eV below the thresholds. (4) The peak widths have a 0.5 eV full width at half maximum. (5) There is only a single isolated peak because the  $\delta$ -function potential supports only one bound state.

\*Present address: University of Texas, Arlington, TX 76019.

<sup>1</sup>J. B. Pendry, *Low Energy Electron Diffraction* (Academic, New York, 1974).

<sup>2</sup>E. G. McRae and C. W. Caldwell, *Surf. Sci.* **7**, 41 (1967).

<sup>3</sup>E. G. McRae, *Surf. Sci.* **49**, 675 (1975); *Rev. Mod. Phys.* **51**, 541 (1979).

<sup>4</sup>J. Rundgren and G. Malmström, *Phys. Rev. Lett.* **38**, 836 (1977); *J. Phys. C* **10**, 4671 (1977).

<sup>5</sup>J. C. Le Bossé, J. Lopez, C. Gaubert, Y. Gauthier, and R. Baudoing, *J. Phys. C* **15**, 3245 (1982).

<sup>6</sup>C. Gaubert, R. Baudoing, and Y. Gauthier, *Surf. Sci.* **147**, 162 (1984).

<sup>7</sup>See for example, A. P. Mills, Jr., in *Positron Solid State Physics*,

edited by W. Brandt and A. Dupasquier (North-Holland, Amsterdam, 1983), p. 432; P. J. Schultz and K. G. Lynn, *Rev. Mod. Phys.* **60**, 701 (1988).

<sup>8</sup>I. J. Rosenberg, A. H. Weiss, and K. F. Canter, *Phys. Rev. Lett.* **44**, 1139 (1980).

<sup>9</sup>M. N. Read, *Solid State Commun.* **47**, 1 (1983).

<sup>10</sup>P. J. Jennings and D. Neilson, *Solid State Commun.* **65**, 649 (1988).

<sup>11</sup>A. P. Mills, Jr. and W. S. Crane, *Phys. Rev. B* **31**, 3988 (1985).

<sup>12</sup>N. W. Ashcroft and N. D. Mermin, *Solid State Physics* (Saunders College, Philadelphia, 1976).

<sup>13</sup>E. G. McRae and R. A. Malic, *Surf. Sci.* **177**, 74 (1986).

<sup>14</sup>K. F. Canter, G. R. Brandes, T. N. Horsky, P. H. Lippel, and

- A. P. Mills, Jr., in *Atomic Physics with Positrons*, edited by J. W. Humberston and E. A. G. Armour (Plenum, New York, 1987), pp. 153–160.
- <sup>15</sup>T. E. Gallon, I. G. Higginbotham, M. Prutton, and H. Tokutaka, *Surf. Sci.* **21**, 224 (1970).
- <sup>16</sup>A. P. Mills, Jr. and W. S. Crane, *Phys. Rev. Lett.* **53**, 2165 (1984).
- <sup>17</sup>P. H. Lippel, Ph.D. thesis, Brandeis University, 1987, available from University Microfilms, Ann Arbor, MI 48109.
- <sup>18</sup>E. M. Gullikson and A. P. Mills, Jr., *Phys. Rev. B* **36**, 8777 (1987).